Cole-Puli International Conference Publishing Group

Science, Engineering and Technology Proceedings

Article

2025 International Conference on Science Technology, Architecture, Power and Intelligent Information Technology (APIIT 2025)

Measurement of Energy Loss and Coefficient of Restitution in Inelastic Collisions Using Tracker and Phyphox

Ruiqi Sha [1,*]

[1] Automatic Control and Systems Engineering, University of Sheffield, Sheffield, s10 2tn, UK
* Correspondence: Ruiqi Sha, Control and Systems Engineering, University of Sheffield, Sheffield, s10 2tn, UK

Abstract: Modern smartphones incorporate a variety of high-precision, highly sensitive sensors, and companion apps are being developed to leverage these capabilities. This experiment explores how the phyphox app can enhance traditional methods for measuring energy loss and the coefficient of restitution during inelastic collisions involving spheres with different elastic properties. Using Tracker's automatic object-tracking and data-analysis tools, we analyze collision videos to investigate how energy loss and restitution vary with the number and type of intermediate layers. Our results indicate that, for spheres of identical elasticity, the residual energy decreases as the number of layers increases and as sphere mass increases, and the coefficient of restitution likewise diminishes with more layers. Under different materials, energy loss and restitution depend on the medium: for example, a table-tennis ball's rebound speed after a given number of bounces decreases with drop height, with the greatest energy retention on a wooden board, then on a concrete floor, and least on an iron plate; its restitution coefficient follows the same order. Comparing spheres of different elasticity, those with higher elastic moduli retain more energy and exhibit higher restitution coefficients. Notably, restitution depends only on the sphere's material, not on its size or mass: both large and small elastic spheres have almost identical restitution values, both exceeding that of the table-tennis ball, while an aluminum sphere shows the lowest restitution.

Keywords: inelastic collisions; coefficient of restitution; energy loss; Tracker

Received: 26 April 2025
Revised: 04 May 2025
Accepted: 16 May 2025
Published: 05 June 2025

1. Introduction

Collisions are ubiquitous in engineering, materials science, and sports, and they provide a key experimental test of the laws of momentum and energy conservation. Depending on energy dissipation, collisions can be classified as perfectly elastic (no energy loss), partially inelastic (some energy dissipated as heat, sound, or deformation), or perfectly inelastic (maximum energy loss). To quantify energy dissipation, physicists use the coefficient of restitution ee, defined as the ratio of post-collision separation speed to pre-collision approach speed; ee depends solely on the materials and surface properties of the colliding bodies. Traditional measurements rely on photoelectric gates or high-precision displacement sensors to capture sphere velocity and position, but such setups are costly and complex to operate. With the ever-improving accuracy of smartphone accelerometers, gyroscopes, and acoustic sensors, high-precision motion measurements can now be performed at minimal cost. The availability of open-source video-analysis software like Tracker, along with multifunctional physics apps such as phyphox, makes this possible even in ordinary classrooms or laboratories. This study combines Tracker's trajectory-

tracking capabilities with phyphox's acoustic timing and inelastic-collision tools. Tracker extracts displacement–time (h–t) and velocity–time (v–t) data from collision videos, while phyphox accurately records the intervals, residual energy, and coefficients of restitution for successive bounces. Together, these methods allow us to examine how sphere elasticity, layer count, and material type affect energy loss and restitution in inelastic collisions [1]. The approach is low-cost, easy to operate, and provides intuitive data visualization, offering a novel experimental framework for university physics teaching and research [2].

2. Research Background

2.1. Topic Motivation

A collision proceeds through compression, maximum deformation, and restitution stages. In a perfectly elastic collision, deformation fully recovers and no energy is lost, yielding e = 1. In a perfectly inelastic collision, deformation is permanent and energy loss is maximal, with e = 0. Most real-world collisions fall between these extremes, exhibiting partial elasticity with $0 < e < 1$. The coefficient of restitution ee reflects the ratio of separation to approach speeds and depends only on the colliding materials and surface characteristics, making it a key parameter for quantifying energy dissipation [3]. By leveraging modern smartphones' high-precision accelerometers and acoustic sensors together with Tracker's video analysis and phyphox's timing modules, this experiment innovatively integrates trajectory analysis and acoustic measurement to study energy loss and restitution in inelastic collisions, offering low cost, high precision, and user-friendly operation [4].

2.2. Experimental Objectives

The goals of this experiment are to master the use of smartphone-embedded sensors and the phyphox app's acoustic stopwatch and inelastic-collision module; to learn how to use Tracker and Excel to track the ball's trajectory in experimental videos, export data, and plot displacement–time (h–t) and velocity–time (v–t) curves; to investigate how the coefficient of restitution of identically elastic spheres varies with the number of intermediate layers; and to analyze how the percentage of residual energy depends on layer count, layer material, sphere mass, and elasticity, thereby providing quantitative insight into the mechanisms of collision energy loss [5].

3. Equipment and Environment

3.1. Experimental Equipment

In order to achieve high precision measurement of the whole process of inelastic collision of elastic balls, this experiment has been carefully configured at the hardware and software level. Firstly, three smart phones were used to complete multi-task collaboration. One of them was fixed on a tripod to record the entire video, ensuring that the shooting angle was aligned to match the coordinate system used in the Tracker software. The other two were used to run phyphox's acoustic stopwatch, which captures the time between two adjacent impacts with 1-millisecond accuracy. They also operated the inelastic-collision module, which directly outputs the percentage of remaining energy and preliminary estimates of the restitution coefficient for each impact [6]. Secondly, after importing the experimental video into a laptop computer equipped with Tracker software, the particles can be tracked manually or semi-automatically, and the displacement–time (h–t) and velocity–time (v–t) data can be exported for cross-validation with phyphox measurements. Third, the experimental table must be level and stable. After accurate correction by the digital level, the black tape is used to calibrate the five falling heights of 30 cm, 40 cm, 50 cm, 60 cm and 70 cm along the vertical direction of the table. In order to reduce calibration error, steel tape and laser ranging are used to check each other for height marking. Fourth, the dielectric layer system uses 70 cm-wide eco-friendly PE tape, stacked into 1 to 6 layers to allow controlled adjustment of the number of damping layers [7]; At the same time,

three material surfaces of wood board, iron plate and ordinary floor are prepared to further study the influence of different hardness on energy dissipation. Finally, the experimental balls include a specially selected table tennis ball (with good consistency and a uniform surface), one large and one small polyurethane elastic ball (with high elasticity and a significant mass difference), and an aluminum ball (with high stiffness and low elasticity). These variations allow for comparative analysis of collision characteristics under different elasticity and mass conditions. The installation and debugging of all equipment strictly refer to the safety regulations, and the function test and error evaluation are carried out before and after the experiment to ensure the reliability and repeatability of the data [8].

3.2. Environmental Conditions

To maximize tracking and acoustic-timing accuracy, all tests are conducted indoors on a flat surface with even, diffuse lighting and minimal background noise. The camera's optical axis must be perpendicular to the drop plane, and the table surface is leveled in advance with a spirit level. Care is taken to keep extraneous objects out of the frame to reduce Tracker's tracking errors and ensure that phyphox captures collision sounds clearly, without interference.

4. Experimental Design and Procedure

4.1. Experimental Principle

The experiment can be divided into two parts: the free fall of the small ball and the inelastic collision, as shown in Figure 1:

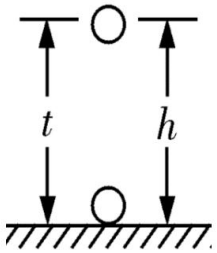

Figure 1. Illustration of the ball falling.

Firstly, when the initial velocity of the ball is zero, the ball falls freely from the calibrated height, ignoring the air resistance, and its motion satisfies the law of uniform acceleration linear motion as shown in Formula 1:

$$h = \frac{1}{2}gt^2$$

Velocity of incidence as shown in Formula 2:

$$v_1 = gt$$

Here, *h* denotes the fall height, *t* is the fall time, and *g* is the gravitational acceleration. Figure 1 visually shows the whole process of the ball falling from the static state to the first impact on the ground, providing a reference frame for time and displacement calibration in the experiment [9]. Secondly, when the ball undergoes an inelastic collision with the surface, it experiences irreversible energy dissipation. The coefficient of restitution is defined as the ratio of the rebound velocity to the incident velocity after the collision, as shown in Formula 3:

$$e = \frac{v_2}{v_1}$$

According to energy conservation, the difference between the gravitational potential energy mgh of the ball at the falling height h and the kinetic energy $\frac{1}{2}mv_2^2$ after collision is the lost energy as shown in Formula 4:

$$W = mgh - \frac{1}{2}mv_2^2$$

In this experiment, the acoustic stopwatch module of phyphox was used to record the time interval T (accuracy up to 1 ms) of the sound generated by two adjacent impacts, and according to the relationship as shown in Formula 5:

$$v = \frac{1}{2}gT$$

The recovery coefficient e and the percentage of energy remaining are obtained by calculating the incident and rebound velocities respectively. In the video analysis part, the ball particles in the experimental video are manually tracked frame by frame by Tracker software, and the displacement–time (h–t) and velocity–time (v–t) data are derived to visually present the motion characteristics before and after collision. Based on the complementary strengths of Tracker and phyphox, the experimental design integrates image analysis with acoustic measurement to enable high-precision and low-cost analysis of inelastic collisions [10].

4.2. Experimental Procedure

Initially, Tracker was used exclusively to analyze the entire bounce trajectory and compute collision parameters from displacement–time data. However, fitting errors due to slight variations in camera angle and calibration markers proved significant. To improve reliability, we integrated phyphox's acoustic stopwatch and inelastic-collision module to measure time and energy parameters directly. Each experimental run consists of five bounces, yielding five measurements of the time interval T and corresponding energy data. The steps are as follows: Select a release height between 30 cm and 70 cm. Conduct three independent trials at each height, recording both the time intervals and residual energies from phyphox. For each trial (five bounces), compute the coefficient of restitution and then average across the five values to obtain a representative e for that condition. Collate the mean coefficients and residual-energy percentages for different layer counts, layer materials, and sphere types in Excel. Use scatter plots and linear or polynomial regression to analyze how these parameters vary with the number of layers, extracting slopes and intercepts that reflect physical properties. Finally, compare Tracker's displacement–time and velocity–time curves against phyphox's acoustic data to assess the combined method's accuracy and applicability. This approach—featuring repeated trials and statistical averaging—ensures that measured inelastic-collision parameters are both reproducible and reliable.

5. Experiment Content

5.1. Experimental Setup

The experimental setup is shown in Figure 2 and is composed of the following components. First, on a flat table corrected for level, five vertical drop heights—30 cm, 40 cm, 50 cm, 60 cm, and 70 cm—are marked using black tape.

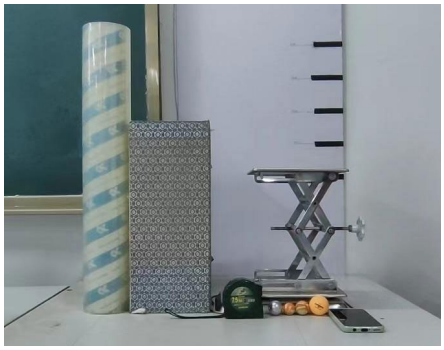

Figure 2. Experimental apparatus.

First, the elastic ball was placed at the marked position, and a consistent release mechanism (either handheld or a simple chute) was used to ensure identical initial conditions for each fall. Thirdly, three smartphones were used to work in parallel -- one was used for HD shooting, the other was running the phyphox acoustic stopwatch module, and the third was running the phyphox inelastic collision module. Finally, 70 cm wide tape with different thickness (1-6 layers) was laid on the table as the medium layer. The same procedure was repeated on both the iron plate and the floor surface as part of the experimental process. The setup was compact, with the camera axis parallel to the surface of the test plate to ensure synchronized image and acoustic data acquisition for accurate alignment and analysis.

5.2. Experimental Procedures

5.2.1. Relationship between Restitution Coefficient and the Number of Media Layers

1). Five falling heights of 30 cm, 40 cm, 50 cm, 60 cm, and 70 cm were calibrated with Five falling heights of 30 cm, 40 cm, 50 cm, 60 cm, and 70 cm were marked with tape on the horizontally leveled table, and three groups of independent experiments were conducted for each height.

2) One to six layers of tape were laid sequentially on the calibrated table surface. For each configuration, tests were conducted using the table tennis ball, large and small elastic balls, and the aluminum ball at the five designated heights. The same procedure was repeated on the iron plate and floor surface.

3) The time interval data of each collision recorded by phyphox acoustic stopwatch and inelastic collision module were respectively exported, and the average time interval of five bouncings at the same height and the same number of media layers was calculated.

4) Calculate the incident velocity and rebound velocity according to the average time interval, then calculate the recovery coefficient, and plot a line graph showing how the coefficient of restitution e varies with the number of media layers X in Excel.

5.2.2. Relationship between Energy Loss and the Number of Media Layers

Under the conditions of the same height, the number of media layers and the sphere, the phyphox inelastic collision module was used to directly obtain the percentage of energy remaining E% after each collision, and the results of multiple experiments under the same condition were averaged, and the relationship curve of the percentage of energy remaining E% with the change of the number of media layers X was drawn in Excel. In order to quantify the impact of the number of dielectric layers on the collision energy loss.

6. Expected Results of the Experiment

According to the previous literature and pre-experimental data, as the number of medium layers X increases, the energy dissipation and damping effect in the collision process will be significantly enhanced, which is shown by the reduction coefficient e and the percentage of energy remaining E% layer by layer. Taking the game-specific table tennis as an example, when the number of media layers increases from 0 to 6, the energy surplus decreases from about 84.50% to 76.80%, with an average decrease of about 1.30 percentage points per layer. The corresponding recovery coefficient decreases from 0.9194 to 0.8769, with an average decrease of about 0.0071 per layer. This linear trend was also observed for large elastic balls (E% decreased from 88.80% to 85.10%, e decreased from 0.9436 to 0.9254) and small elastic balls (E% decreased from 86.20% to 85.20%, e decreased from 0.9376 to 0.9295). However, the decrease is slightly different: about 0.62 percentage points per layer for the large elastic ball, and about 0.17 percentage points per layer for the small elastic ball, reflecting the influence of the elastic coefficient and mass of the ball on the sensitivity of energy loss.

In the extreme case, with only a slight absolute decrease, but a relatively large percentage change compared to its already low initial value. The coefficient of restitution

decreases from 0.1400 to 0.1359, indicating that is mainly manifested as deformation loss and acoustic vibration dissipation, rather than contributing to rebound height or velocity. The impact of different media types on the collision characteristics is also significant. Taking table tennis as an example, under the condition of 30 cm falling height and the same number of media layers, the energy residual of wood media changes most dramatically (about 70.3%-61.5%), followed by floor media (about 68.9%-63.6%), and iron plate media is the smoothest (about 69.7%-63.5%). The corresponding coefficient of restoration decreases from 0.9194 to 0.9088 on board, from 0.9174 to 0.9141 on floor, and from 0.9194 to 0.9061 on iron plate. Analysis of the slope and intercept suggests that the damping effect of the wood medium is strongest, while that of the iron plate is the weakest. Based on the above expected results, it can be concluded that the recovery coefficient ee and the energy residual E% are linearly decreasing with the number of dielectric layers, and the slope varies with the elastic coefficient and mass of the sphere. The spheres with higher elasticity and mass have higher initial e and E% values, but the absolute decrease with the increase of the number of layers is smaller. In terms of energy dissipation, the slopes for different materials follow the order: wood > floor > iron plate, indicating that damping and friction dissipation effects are closely related to the material of the medium. High stiffness spheres such as aluminum spheres exhibit extremely low rebound performance, but the relative variation of e and E% can still reflect the cumulative effect of the number of dielectric layers on energy dissipation. The above expectations will assist the fitting analysis of images and data in subsequent experiments, provide a quantitative basis for the energy loss mechanism of inelastic collisions, and serve as a reference for the design and optimization of instructional physics experiments.

7. Experimental Data and Result Processing

7.1. Experimental Raw Data

All the original observation data of this experiment, including different spheres (table tennis ball, large elastic ball, small elastic ball, aluminum ball) under five combinations of falling heights (30 cm, 40 cm, 50 cm, 60 cm, 70 cm) and multi-layer media (0-6 layers of tape, wood, iron plate, floor), The percentage of energy remaining for each collision versus the collision time interval recorded by the acoustic stopwatch. The original data table is arranged by a four-level index of sphere, medium type, medium layer number and falling height to facilitate subsequent screening and processing. See Appendix 1 for details.

7.2. Experimental Data Processing

For the five bouncing processes under each group of conditions, the incident velocity and rebound velocity were calculated by using the time interval the time interval T measured by the acoustic stopwatch. The arithmetic average of the five calculation results under the condition of the same number of media layers and the same falling height was obtained, and the average recovery coefficient under the conditions was obtained. According to the percentage of energy remaining after each collision directly output by the inelastic collision module, multiple measurements under the same experimental condition are accumulated and averaged to obtain the average energy remaining E% representing the condition. The average restitution coefficient and average energy residual data of all spheres in different media layers and different materials were imported into Excel, and scatter plots of e vs. X and $E\%$ vs. X were generated, where X was the number of media layers or the type of media code. Through linear regression fitting, the slope and intercept of the fitting line are extracted. The slope reflects the attenuation rate of the restitution coefficient or energy residual with the increase of the number of damping layers of the medium, which can quantify the strength of the medium to energy dissipation. The intercept corresponds to the initial e or E% level at X=0, with no dielectric layer. Combining the fitting results with the physical meaning, the influence of different elasticity and mass

of the sphere and different media materials on the collision loss characteristics can be intuitively compared.

8. Use Tracker

8.1. H-T Curve Generation and Analysis

In Tracker software, two sets of videos of ping-pong balls, large elastic balls, small elastic balls and aluminum balls falling at a height of 30 cm were imported: one with no dielectric layer (0 layer of tape) and the other with six layers of tape medium. By establishing a vertical coordinate system in the Tracker and manually tracking the ball particle, the height-time (H-T) curve of each bounce can be obtained.

Taking table tennis as an example, it can be observed in Figure 3 and Figure 4 that in the same time interval, the bouncing cycle of the small ball is longer and the number of bounces is higher when there is no medium. However, under the condition of six-layer medium, the interval between peaks and valleys of the curve is significantly shortened, and the number of bouncings in the same time is increased, which indicates that the damping effect of the medium is enhanced and the energy is dissipated faster. Comparing the H-T curves of the four kinds of spheres, it can also be found that the large and small elastic balls with larger elastic coefficients have longer bounce periods and higher peak positions under the same medium conditions. the aluminum ball, characterized by the highest stiffness and lowest elasticity has the shortest period and the smallest amplitude in the two sets of curves, reflecting its extremely low rebound ability and high energy loss.

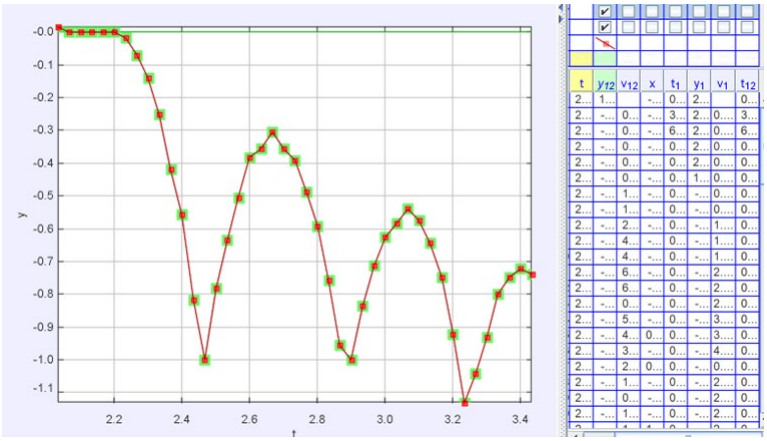

Figure 3. Table tennis ball at 30cm height without medium fall.

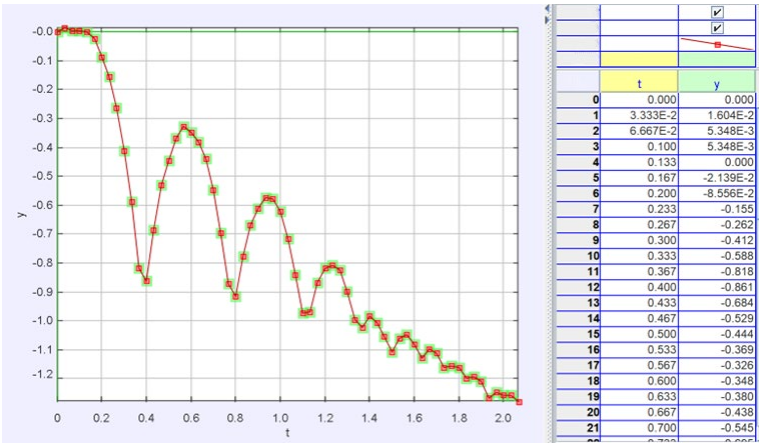

	t	y
0	0.000	0.000
1	3.333E-2	1.604E-2
2	6.667E-2	5.348E-3
3	0.100	5.348E-3
4	0.133	0.000
5	0.167	-2.139E-2
6	0.200	-8.556E-2
7	0.233	-0.155
8	0.267	-0.262
9	0.300	-0.412
10	0.333	-0.588
11	0.367	-0.818
12	0.400	-0.861
13	0.433	-0.684
14	0.467	-0.529
15	0.500	-0.444
16	0.533	-0.369
17	0.567	-0.326
18	0.600	-0.348
19	0.633	-0.380
20	0.667	-0.438
21	0.700	-0.545

Figure 4. ping-pong ball when the height six layer medium falls.

8.2. V-T Image Rendering and Analysis

Based on the same batch of videos, the velocity-time (V-T) data were exported from Tracker, and the V-T curves of four kinds of spheres under 0 layer and 6 layer media were plotted respectively.

Taking table tennis as an example, as shown in Figure 5 and Figure 6, the V-T curve shows that under the condition of no medium, the peak rebound speed after collision is higher, and the fall speed is also faster. However, in the six-layer medium, the peak velocity decreases significantly, and the downward slope becomes less steep, indicating that the kinetic energy of the ball is absorbed by the medium layer to a greater extent after collision. Compared with different spheres, the V-T peak value of the elastic ball is relatively higher and the attenuation speed is slower, which indicates that the elastic ball has good elasticity and less energy dissipation. The aluminum sphere has the lowest peak value and the fastest attenuation, confirming its high energy loss in inelastic collisions. Through these V-T curves, we can intuitively quantify the inhibitory effect of the increase of the dielectric layer on the rebound velocity, and further confirm the law of the decreasing of the restitution coefficient and the energy residual with the increase of the dielectric damping.

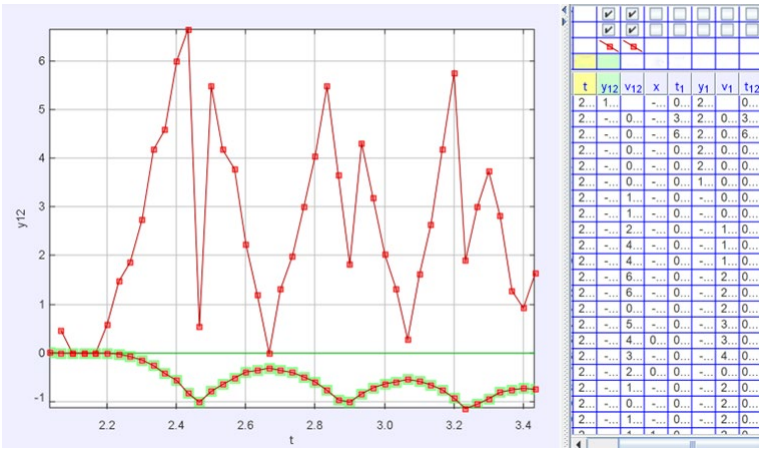

Figure 5. table tennis ball at 30 cm height without medium fall.

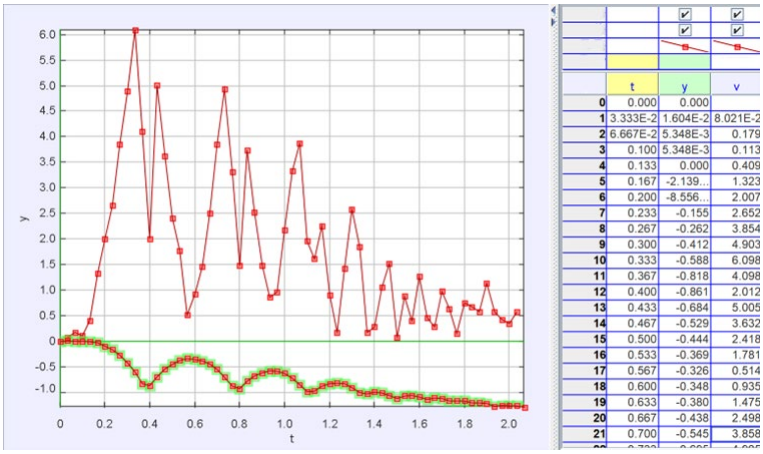

Figure 6. ping-pong ball when six layers of medium fall at 30 cm height.

9. Experimental Conclusion

Through the comprehensive study of the experimental data and Tracker image analysis results of the repeated bouncing of different spheres under multi-layer media and multi-material surfaces, we draw the following main conclusions:Firstly, under the condition of small balls with the same elastic coefficient, the energy remaining percentage E%

after collision shows a significant downward trend with the increase of the number of medium layers, whether it is a ping pong ball, a large elastic ball or a small elastic ball. The results show that the more layers of the medium, the more serious the inelastic dissipation during the collision, and more kinetic energy is lost in the form of heat, sound and deformation energy. At the same time, the coefficient of restitution ee also decreases, indicating that the ratio of the rebound velocity of the ball leaving the medium surface to the incident velocity decreases continuously, which weakens the rebound performance. After in-depth comparison, it is also found that when the mass of the sphere is larger, the E% value of the medium with the same number of layers is relatively slightly lower, which means that under the same damping conditions, the heavy sphere is more likely to consume more energy in the medium by friction or adhesion.

10. Conclusion

Based on the traditional inelastic collision measurement method, this experiment realized a number of innovations and optimizations. For the first time, the acoustic stopwatch and inelastic collision module of the mobile phone application phyphox were synchronized with the image tracking function of Tracker, so as to obtain the collision energy loss and motion trajectory data at the same time. Through the flat throwing experiment design and multi-layer medium scheme, the manual release error is effectively reduced and the influence of the ball mass on the recovery coefficient and energy residual is verified. In the optimization process, we proposed to improve the shooting Angle, introduce an automatic release device, use a flat board instead of tape stacking, and refine the 5 cm height gradient and increase the number of experiments to significantly improve the experimental repeatability and data reliability. This method has both low cost and high operability, and can be extended to physical experiment teaching in secondary and higher schools. Smart phones and open source software are used to help students quickly measure and analyze collision parameters, and at the same time cultivate their practical ability and data processing literacy. Secondly, in terms of medium types, the experimental results show that the wood medium has the strongest inhibitory effect on energy loss, followed by the floor, and the iron plate has the weakest effect on energy loss. Under the condition of the same falling height and collision times, the average energy residual of the ping pong ball on the surface of the board is the least, and the restitution coefficient decreases the most. However, on the surface of the iron plate, the energy residual remains at a high level, and the change of restitution coefficient is minimal. This phenomenon reflects that the hardness and surface elasticity of the medium material have a significant impact on the collision loss mechanism: the lower the hardness (such as wood), the more obvious the deformation energy absorption, and the more energy dissipation. The higher the hardness (such as iron plate), the less energy absorption of deformation, the higher rebound efficiency. Finally, when comparing the spheres with different elastic coefficients, we find that the small spheres with higher elastic coefficients (large and small elastic spheres) not only have higher restitution coefficients and energy surplus, but also have slower decay rate under the condition of no dielectric layer. This indicates that the high elastic material can more effectively restore the deformation energy to kinetic energy, so as to improve the rebound performance after collision. On the other hand, the coefficient of restitution and energy residual of the high stiffness and low elastic sphere, such as aluminum ball, are significantly lower. These values are almost unaffected by the sphere's mass and are mainly determined by the material's elastic modulus. It is worth noting that the restitution coefficients of the large elastic ball and the small elastic ball are basically consistent, which further verifies that the restitution coefficient is only related to the material properties and is independent of the sphere size or mass. In summary, through the measurement and analysis method combining smart phone and open source software, this experiment systematically quantifies the joint mechanism of the number of media layers, the type of materials and the elasticity of the sphere on the energy loss and recovery performance in

inelastic collision, which provides new experimental ideas and data support for physics teaching and related engineering applications.

Appendix 1. Raw Experimental Data

Residual Energy of a Ping-Pong Ball on Different Media.

Medium	30 cm	40 cm	50 cm	60 cm	70 cm
Wooden board	70.3 %	68.9 %	67.8 %	63.5 %	61.5 %
Iron plate	69.7 %	68.2 %	64.7 %	65.2 %	63.5 %
Concrete floor	68.9 %	69.2 %	66.8 %	65.1 %	63.6 %

Collision Time of a Ping-Pong Ball on Different Media (Time between successive impacts, in seconds).

Medium	30 cm	40 cm	50 cm	60 cm	70 cm
Concrete floor	0.455	0.524	0.585	0.640	0.687
Wooden board	0.455	0.525	0.586	0.639	0.685
Iron plate	0.454	0.524	0.586	0.641	0.691

Residual Energy of a Ping-Pong Ball vs. Number of Layers.

Layers	30 cm	40 cm	50 cm	60 cm	70 cm
0	84.50 %	84.30 %	84.10 %	83.80 %	82.60 %
1	83.20 %	83.10 %	81.10 %	83.80 %	81.50 %
2	82.20 %	80.20 %	80.60 %	82.70 %	79.60 %
3	80.60 %	80.20 %	79.90 %	80.80 %	79.70 %
4	79.50 %	79.80 %	79.10 %	78.80 %	77.70 %
5	77.90 %	78.50 %	78.60 %	77.50 %	77.20 %
6	76.80 %	76.30 %	77.60 %	77.10 %	75.40 %

Collision Time of a Ping-Pong Ball vs. Number of Layers (Time between successive impacts, in seconds).

Layers	30 cm	40 cm	50 cm	60 cm	70 cm
0	0.455	0.525	0.586	0.641	0.685
1	0.451	0.521	0.576	0.641	0.684
2	0.449	0.513	0.572	0.637	0.675
3	0.445	0.512	0.568	0.627	0.672
4	0.442	0.508	0.571	0.619	0.667
5	0.437	0.505	0.566	0.618	0.665
6	0.434	0.499	0.561	0.617	0.659

Residual Energy of a Large Rubber Ball vs. Number of Layers.

Layers	30 cm	40 cm	50 cm	60 cm	70 cm
0	88.80 %	88.70 %	87.20 %	87.70 %	87.30 %
1	87.10 %	87.00 %	86.60 %	86.00 %	85.80 %
2	87.40 %	85.90 %	85.30 %	85.60 %	84.90 %
3	86.40 %	85.30 %	85.00 %	84.80 %	84.00 %
4	85.90 %	83.10 %	84.20 %	83.50 %	82.80 %
5	85.40 %	82.90 %	82.00 %	82.80 %	82.80 %

6	85.10 %	82.50 %	81.90 %	81.30 %	81.40 %

Collision Time of a Large Rubber Ball vs. Number of Layers (Time between successive impacts, in seconds).

Layers	30 cm	40 cm	50 cm	60 cm	70 cm
0	0.467	0.538	0.598	0.655	0.707
1	0.462	0.533	0.593	0.651	0.699
2	0.463	0.529	0.589	0.647	0.695
3	0.460	0.526	0.590	0.643	0.691
4	0.459	0.522	0.584	0.639	0.689
5	0.457	0.519	0.578	0.636	0.688
6	0.458	0.520	0.579	0.633	0.683

Residual Energy of a Small Rubber Ball vs. Number of Layers.

Layers	30 cm	40 cm	50 cm	60 cm	70 cm
0	86.20 %	88.10 %	87.90 %	86.90 %	86.20 %
1	88.80 %	87.20 %	84.50 %	86.40 %	85.80 %
2	87.30 %	87.40 %	87.50 %	85.80 %	84.50 %
3	87.20 %	87.00 %	86.10 %	84.90 %	83.00 %
4	86.60 %	86.00 %	85.60 %	84.00 %	84.50 %
5	85.40 %	85.40 %	84.70 %	84.80 %	84.30 %
6	85.20 %	86.10 %	85.60 %	83.90 %	83.50 %

Collision Time of a Small Rubber Ball vs. Number of Layers (Time between successive impacts, in seconds).

Layers	30 cm	40 cm	50 cm	60 cm	70 cm
0	0.464	0.536	0.599	0.650	0.702
1	0.467	0.533	0.587	0.651	0.697
2	0.466	0.535	0.593	0.649	0.694
3	0.464	0.534	0.591	0.645	0.688
4	0.459	0.531	0.593	0.640	0.696
5	0.461	0.527	0.589	0.646	0.693
6	0.460	0.530	0.592	0.644	0.688

Residual Energy of an Aluminum Sphere vs. Number of Layers.

Layers	30 cm	40 cm	50 cm	60 cm	70 cm
0	1.97 %	1.70 %	1.56 %	1.48 %	1.44 %
1	1.95 %	1.67 %	1.55 %	1.47 %	1.43 %
2	1.94 %	1.65 %	1.54 %	1.46 %	1.41 %
3	1.91 %	1.64 %	1.52 %	1.46 %	1.40 %
4	1.90 %	1.62 %	1.50 %	1.44 %	1.39 %
5	1.89 %	1.61 %	1.49 %	1.42 %	1.37 %
6	1.85 %	1.60 %	1.47 %	1.41 %	1.36 %

Collision Time of an Aluminum Sphere vs. Number of Layers (Time between successive impacts, in seconds).

Layers	30 cm	40 cm	50 cm	60 cm	70 cm
0	0.0693	0.0741	0.0798	0.0854	0.0910

1	0.0691	0.0738	0.0796	0.0851	0.0904
2	0.0689	0.0735	0.0792	0.0847	0.0898
3	0.0685	0.0731	0.0788	0.0848	0.0896
4	0.0682	0.0728	0.0783	0.0841	0.0892
5	0.0678	0.0725	0.0779	0.0836	0.0887
6	0.0673	0.0723	0.0775	0.0831	0.0883

References

1. H. Hernandez, "Expected Momentum and Energy Changes during Elastic Molecular Collisions," *ForsChem Res. Rep.*, vol. 5, pp. 2020-13, 2020, doi: 10.13140/RG.2.2.26182.09288.
2. H. Hernandez, "Confusion and illusions in collision theory," *ForsChem Res. Rep.*, vol. 8, no. 15, pp. 1–42, 2023, doi: 10.13140/RG.2.2.24913.10088.
3. A. N. Zinoviev, P. Y. Babenko, D. S. Meluzova, and A. P. Shergin, "Contribution of molecular orbital promotion to inelastic energy losses in ion-solid collisions," *Nucl. Instrum. Methods Phys. Res. B*, vol. 467, pp. 140–145, 2020, doi: 10.1016/j.nimb.2019.12.002.
4. F. Salvat, L. Barjuan, and P. Andreo, "Inelastic collisions of fast charged particles with atoms: Bethe asymptotic formulas and shell corrections," *Phys. Rev. A*, vol. 105, no. 4, p. 042813, 2022, doi: 10.1103/PhysRevA.105.042813.
5. M. Nakamura, "Profile of Energy Loss Spectrum in Impulsive Ion Collisions with Heteronuclear Diatomic Molecules: Effects of Mass Asymmetry in Target Molecule," *J. Phys. Soc. Jpn.*, vol. 91, no. 5, p. 054301, 2022, doi: 10.7566/JPSJ.91.054301.
6. S. Acharya et al., "Production of charged pions, kaons, and (anti-) protons in Pb-Pb and inelastic pp collisions at $\sqrt{S_{NN}} = 5.02$ TeV," *Phys. Rev. C*, vol. 101, no. 4, p. 044907, 2020, doi: 10.1103/PhysRevC.101.044907.
7. O. Bünermann, A. Kandratsenka, and A. M. Wodtke, "Inelastic scattering of H atoms from surfaces," *J. Phys. Chem. A*, vol. 125, no. 15, pp. 3059–3076, 2021, doi: 10.1021/acs.jpca.1c00361.
8. D. N. Le and H. T. Nguyen-Truong, "Analytical formula for the electron inelastic mean free path," *J. Phys. Chem. C*, vol. 125, no. 34, pp. 18946–18951, 2021, doi: 10.1021/acs.jpcc.1c05212.
9. P. Pan, M. Debiossac, and P. Roncin, "Polar inelastic profiles in fast-atom diffraction at surfaces," *Phys. Rev. B*, vol. 104, no. 16, p. 165415, 2021, doi: 10.1103/PhysRevB.104.165415.
10. T. Yang, Y. Zhong, Q. Tan, Q. Huang, and X. Gong, "Inelastic collision effects of high-energy neutrons in tungsten materials," *J. Nucl. Mater.*, vol. 569, p. 153934, 2022, doi: 10.1016/j.jnucmat.2022.153934.